

Flashover of Smooth and Knurled Dielectric Surfaces in Dry Air

R. W. Macpherson, *Member, IEEE*, M. P. Wilson, *Member, IEEE*, I. V. Timoshkin, *Senior Member, IEEE*, M. J. Given, *Senior Member, IEEE* and S. J. MacGregor, *Senior Member, IEEE*

Abstract— In pulsed power engineering, solid spacers are used to insulate high voltage parts from extraneous metal parts, providing electrical insulation as well as mechanical support. The breakdown/flashover voltage, at which a discharge process initiates across the solid/air interface, is important in the design process, as it informs designers of specific threshold 'failure' voltages of the insulation system. In this paper, a method to potentially increase the failure voltage, tested under multiple environmental conditions, without increasing the length of the solid spacer, was investigated. Three dielectric materials: HDPE (high-density polyethylene), Ultem (polyetherimide) and Delrin (polyoxymethylene), were tested under a 100/700 ns impulse voltage. Cylindrical spacers made of these materials were located in the centre of a plane-parallel electrode arrangement in air, which provided a quasi-uniform electric field distribution. Breakdown tests were performed in a sealed container at air pressures of -0.5, 0 and 0.5 bar gauge, with a relative humidity (RH) level of <10%. The materials were tested under both, negative and positive polarity impulses. The surfaces of a set of solid spacers were subjected to a 'knurled' finish, where ~0.5 mm indentations are added to the surface of the materials, prior to testing, to allow comparison with the breakdown voltages for samples with 'smooth' (machined) surface finishes. The results show that the flashover voltage can be increased by the addition of a spacer with a knurled surface, by up to 60 kV under certain conditions, in comparison to a 'smooth' (machined) surface finish.

Index Terms— Dielectrics, Flashover, Gas Insulation, Knurled insulation, High Voltage, Impulse Testing, Insulation Testing, Nano-second Impulse, Profiled Insulation, Pulsed Power, Surface Modification

I. INTRODUCTION

Within pulsed power systems, the governing factor determining the overall breakdown strength of the system is often the voltage that initiates flashover, in the vicinity of solid insulating parts required to provide mechanical support. In this work, the application of geometric modifications to the surfaces of solid spacer materials at varying levels of air pressure was investigated, in order to quantify the effect that the modified surface finish has on the flashover voltage of the insulation system. This is particularly important for pulsed power devices that are subject to air pressure fluctuations. The main parameters that govern the flashover process in the dry conditions used in this paper are the

material properties, material surface, electrode-spacer arrangement, and pressure.

Characterising the effect of the introduction of modifications to spacer surfaces, whether achieved by simple roughening of the surface using sandpaper in 1980, [1], or via a more intricate PIII processing system in 2020, [2], has been an engineering challenge for many years, with designers attempting to increase the hold-off voltages of their insulation systems by means other than simply increasing the length of the spacer. Another common method of increasing the hold-off voltage is to modify the insulator geometry, to increase the path length that the discharge channel must traverse during the flashover process [3-8].

In this work, a novel 'knurling' method was implemented, to modify the surface of the insulator with set ~0.5 mm indentations across the spacer surface. This manufacturing process provided a quick, consistent way of modifying a dielectric surface, with a view to increasing the flashover voltage, without increasing the length of the spacer.

Previous work on roughened/manipulated dielectric surfaces is detailed in [9]. The authors investigated the effect of modifying a dielectric surface using a sandblasting method, yielding surface roughness in the range 5 – 10 μm , within a SF_6/N_2 environment, under DC voltage. The authors found that, with an increasing surface roughness, the flashover voltage was increased by up to 13.3% for positive applied voltage, and by up to 24.7% for negative voltages. The authors proposed that higher levels of surface roughness resulted in reduced probability of secondary electron emission, and higher breakdown voltage.

A study of the effect of the surface roughness of solid support insulators in an SF_6 environment was published in [10]. The barrel-shaped support insulators, made of epoxy resin with embedded copper connectors on both sides, were placed in a rod-plane electrode system, with the HV rod in contact with the upper connector, and the lower connector resting on the grounded metal plane. Lightning impulse flashover tests were conducted on insulators with varying surface roughness, and with varying gas pressure in the test cell. A decrease in the flashover voltage with an increase in the average surface roughness, R_a , was observed: the flashover voltage was highest for new, untreated, samples with $R_a \sim 0.1 \mu\text{m}$; however, as R_a was increased from $\sim 0.1 \mu\text{m}$ to $\sim 1.4 \mu\text{m}$ (for samples treated with sandpaper), the flashover voltage decreased by $\sim 2\%$ under positive polarity and by $\sim 6\%$ under negative polarity.

The work of Ruairidh W Macpherson was supported in part by the Engineering and Physical Science Research Council (EPSRC) under Grant EP/N509760/1. (Corresponding author: Ruairidh W Macpherson). The authors are with the Department of Electronic and Electrical Engineering, High Voltage Technologies Research Group, University of

Strathclyde, G1 1XQ Glasgow, U.K. (e-mail: ruairidh.macpherson@strath.ac.uk)..

Color versions of one or more of the figures in this article are available online at <http://ieeexplore.ieee.org>

The authors of [11] detail the effect of the inclusion of surface deviations with larger dimensions, where different spacer geometries are proposed, rather than subjecting the surfaces of cylindrical spacers to a roughening process. The authors concluded that the shape of spacer used in their study (cylindrical, concave and umbrella-shaped) largely affects the flashover process due to variation in the level of accumulated charge which is deposited on the spacer surface.

In this paper, a combination of these surface modification processes is adopted, adding surface ‘roughness’ via a manufacturing process. Cylindrical insulating spacers, in the form of rods 40 mm in length and 30 mm in diameter, were produced with a novel ‘knurled’ insulator surface finish, to enable comparison with the breakdown behaviour of samples with a smooth (machined) insulator surface finish. The knurled surface finish consists of diamond-shaped indentations, machined on to the surface of the materials.

Experimental data has been generated on the flashover voltages of samples of three solid materials, HDPE (high-density polyethylene), Ultem (polyetherimide) and Delrin (polyoxymethylene). All tests were conducted at a relative humidity (RH) level of <10%, and at pressures of -0.5, 0 and 0.5 bar gauge. Samples were subjected to negative and positive-polarity impulsive voltages from a 10-stage Marx generator with an erected capacitance of 8 nF, generating a 100/700 ns voltage wave- shape, 100 ns, 0 - 100% front time, and 700 ns, 50% to the half-peak voltage for the fall time. The relative permittivity of each of the materials was $\epsilon_r = 2.3$ for HDPE, $\epsilon_r = 3.0$ for Ultem, and $\epsilon_r = 3.8$ for Delrin. All tests were conducted at ambient laboratory temperature of ~ 23 °C.

Twenty breakdown events were recorded for each set of conditions, and the U_{50} (median) flashover initiation voltages were determined from the 20 resulting breakdown waveforms from each test. The U_{50} flashover voltages of samples of the three different materials were then compared with each other, and with baseline values for open air gaps, for different surface finishes; different pressures; and for both, negative and positive, polarity; with a view to characterising any synergistic effects.

II. METHODOLOGY

A. Experimental Arrangement

The electrode-spacer configuration is illustrated Fig. 1a. This arrangement includes two parallel polished stainless-steel disk electrodes, with radius $R1 = 40$ mm. The radius of the curved edges is $R2 = 10$ mm. In each test, a cylindrical dielectric spacer was placed between the electrodes (the radius of the solid cylinder is $R3 = 15$ mm, and its length is $L = 40$ mm). The upper electrode was connected to either positive or negative HV, and the lower electrode was grounded. The electrode-insulator assembly was housed within a sealed test chamber, to facilitate changing of the internal air pressure.

The electrode topology resulted in a quasi-uniform electric field distribution during energisation, shown from the axisymmetric field simulation in Fig. 1b, creating a weakly non-uniform electric field distribution, with an increase in the field intensity of $\sim 87\%$ at the rounded edge of the HV electrode as compared with the field at the rounded edge of the ground

electrode. The simulation incorporates the Laplacian equation: $\nabla^2 V = 0$, and a Dirichlet boundary condition of $V = 0$ was used to simulate the effects of measured distances to grounded parts of the Faraday test cage from where the test cell was located. This resulted in an asymmetric electric field distribution, prompting both impulse polarities to be tested.

The electric field at the HV electrode was found to depend on the angle between the electrode and the surface of the solid dielectric at the triple junction point (TJP). In an open-air gap (no solid spacer), as well as in air-solid insulation systems where the angle between the electrode and solid dielectric was 90° (dielectric surface normal to the electrode surface), the highest electric field was at the rounded electrode edge. In such cases with smooth (machined) surfaces, the electric field at the TJP was $\sim 48\%$ lower than the field at the rounded electrode edge for all three solid materials, as shown in Fig. 2. Reduction of the contact angle through knurling was shown to increase the electric field intensity at the TJP, referenced to that at the electrode edges, as seen in Fig. 2.

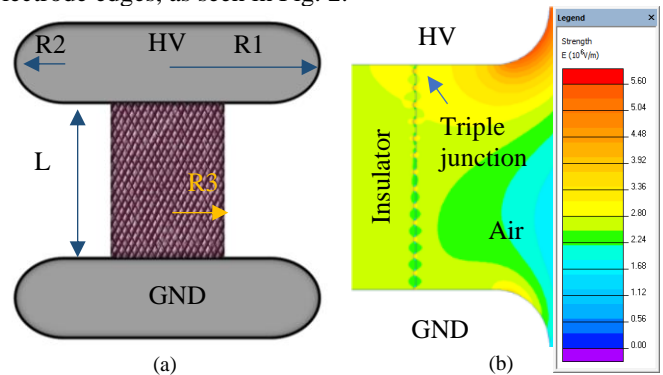


Fig. 1. a) Parallel-plane electrode configuration, with added dielectric spacer with knurled surface and b) Electrostatic field simulation of knurled spacer. The applied voltage was 100 kV, and the relative permittivity of the dielectric sample was 3. Boundary conditions (not shown due to the long distances involved) are at 1.5 m from the electrode edges to the side wall of the lab (r direction), and at 1.25 m from the electrodes to the lab ceiling (z direction), which correspond to the physical distances in the Faraday caged test lab.

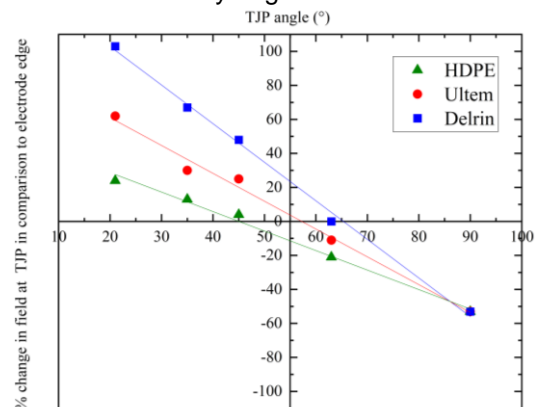


Fig. 2. Percentage change of TJP electric field strength compared to field at electrode edge at TJP contact angles of 21° , 35° , 45° , 63° and 90° , linear distributions added to show performance of each material with changing TJP angle.

Plotted in Fig. 2 are the percentage changes in the simulated maximum field strength values at the TJP, compared to that at the rounded electrode edge, at contact angles of 21°, 35°, 45°, 63° and 90°. As expected, as the TJP contact angle decreased, the field increased. Ultimately, using an iterative approach in additional electrostatic field simulations, the threshold contact angles at which the field at the TJP will exceed that at the rounded electrode edge were found to be 45° for a knurled HDPE surface, 56° for a knurled Ultem surface, and 65° for a knurled Delrin surface.

The insulation system was designed for use nominally at atmospheric pressure; however, HV tests were conducted at -0.5, 0 and 0.5 bar gauge, in order to quantify the effect of pressure fluctuations either side of atmospheric pressure. A detailed description of the methodology and testing procedures, based on the ‘step up’ procedure detailed in the ASTM D3426-97 standard [12], can be found in [13]. A new spacer was used for each set of 20 flashover events, in order to avoid changes in breakdown behaviour due to material degradation from successive flashover events. Due to the ‘step-up’ testing procedure being used for these tests, breakdown/flashover was always initiated on the falling edge of the waveform, an example of this is shown in Fig. 3. In accordance with [12], the peak applied voltage (see Fig. 3) was recorded as the breakdown/flashover voltage for all tests.

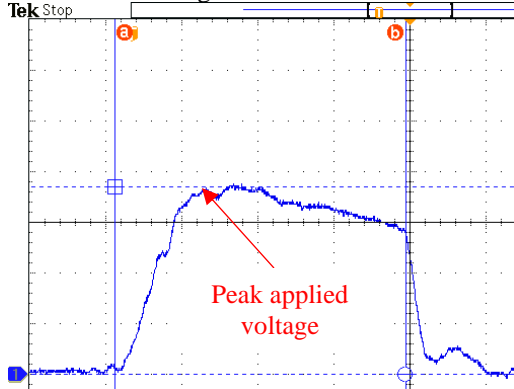


Fig. 3. Example of an output voltage waveform at breakdown, showing the peak applied voltage and the time to breakdown. x-axis time 100 ns/div and y-axis 40.7 kV/div. Smooth HDPE spacer at 0.5 bar gauge. Specific shot shows 150.6 kV flashover and 382 ns time to flashover.

The 2-parameter Weibull distribution was used in the statistical analysis of the obtained results. The probability density function (PDF) of this distribution is given by (1):

$$f(V) = \frac{\beta}{\alpha} \left(\frac{V}{\alpha}\right)^{\beta-1} e^{-\left(\frac{V}{\alpha}\right)^\beta} \quad (1)$$

and the corresponding cumulative distribution function (CDF) is given by (2), [14]:

$$F(V) = 1 - e^{-\left(\frac{V}{\alpha}\right)^\beta} \quad (2)$$

The 20 breakdown voltage values obtained for each set of test conditions were used in the statistical analysis, performed using Microsoft Excel software. To find the α and β values of the 2-parameter Weibull distribution for each dataset, (2) was linearised to the form, $\ln[-\ln(1 - F(V))] = \beta \ln(V) -$

$\beta \ln(\alpha)$, and $\ln[-\ln(1 - F(V))]$ versus $\ln(V)$ was plotted. The shape (α) and scale (β) parameters were then calculated, where β corresponds to the gradient of the straight line, and $\alpha = e^{-\left(\frac{c}{\beta}\right)}$, where c is the intercept value. The obtained α and β values were used to plot synthetic PDFs, and CDFs (1) and (2) for each set of experimental data. The U_{50} breakdown/flashover initiation voltage, which is defined as the median voltage value of the CDF, using (2), was obtained for each series of tests.

For each test, to show the spread in the obtained flashover voltage values, the voltage interval where $\sim 95.4\%$ of data-points reside (95.4% voltage spread interval) was measured using (1), by identifying the point of intersect of this PDF with the negative skewness. By identifying the 2.3% and 97.7% probability values on the CDF, the end points of these voltage intervals are presented as asymmetrical error bars for each U_{50} value. Fig. 4 shows examples of skewed PDFs of breakdown voltage data for Ultem spacers, tested under positive polarity. The solid vertical lines on each PDF represent the U_{50} (median) values, and the dashed lines represent the locations of the upper (right) 97.7% and lower (left) 2.3% end points of the 95.4% voltage spread interval.

At 0.5 bar gauge, there is no overlap of the end points of the 95.4% voltage spread intervals (no overlap of error bars of these two median flashover voltages) for a smooth (blue) Ultem surface and a knurled (red) Ultem surface, as shown in Fig. 4a. However, at -0.5 bar gauge, a clear area of overlap exists between the two 95.4% voltage spread intervals for a smooth (blue) Ultem surface and knurled (red) Ultem surface, as shown in Fig. 4b.

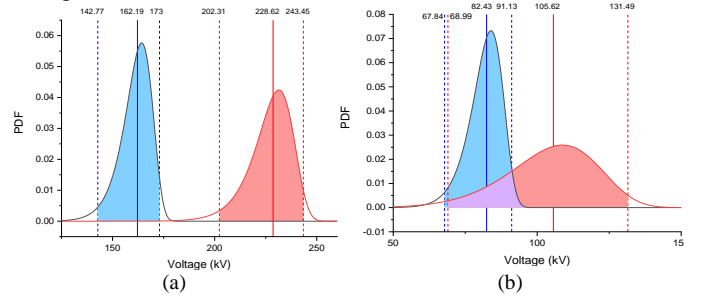


Fig. 4. Example of skewed probability density functions obtained using (1), based on breakdown voltages for Ultem spacers tested under positive polarity, showing a) no error bar overlap (0.5 bar) and b) error bar overlap (-0.5 bar).

The results reported throughout this paper are compared on the basis of skewed error bars, in accordance with the process illustrated in Fig. 4, for all compared tests.

B. Dielectric Surface Characteristics

As aforementioned, the cylindrical spacers were all 40 mm in length and 30 mm in diameter. Samples of each of the three materials, with two different types of surface finish, were prepared and tested. Firstly, samples of each material with a smooth (machined) surface finish were tested (Fig. 5a). The second type of surface finish was ‘knurled’, using a turning method where consistent patterns can be indented onto the surface of a material. This process is commonly used on metals, but was adopted here in order to indent the surfaces of the

dielectric materials, as shown for the example Ultem spacer in Fig. 5b. The knurling method can be considered to be a more intrusive method than introducing surface roughness through abrasion and was used to modify the surface without significantly changing the overall shape of the spacer and, therefore, without affecting the mechanical properties. The surface contains 14, ~ 0.5 mm indentations in a column along the (40 mm) length of the sample surface. The distance between each indentation on each column is ~ 2.85 mm. The helix angle characterising the knurl was $\sim 30^\circ$.

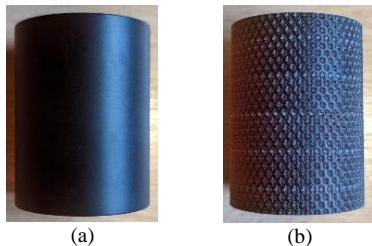


Fig. 5. a) Smooth (machined) Ultem spacer surface; and b) Knurled surface deviations on Ultem spacer surface.

Overall, the knurling method offers the manufacturing advantage of providing a quick, cheap, and consistent way of modifying the surfaces of materials.

III. RESULTS

Fig. 6 shows the graphical data describing the breakdown behaviour of the insulation systems, incorporating spacers with either a smooth or a knurled surface finish, at $<10\%$ RH, showing the U_{50} flashover voltages from 20 flashover events, with the error bars representing the area where $\sim 95.4\%$ of data-points reside.

In Figs. 6a, 6b and 6c, the U_{50} flashover voltages are shown, for air pressures of -0.5 bar gauge, 0 bar gauge, and 0.5 bar gauge, respectively.

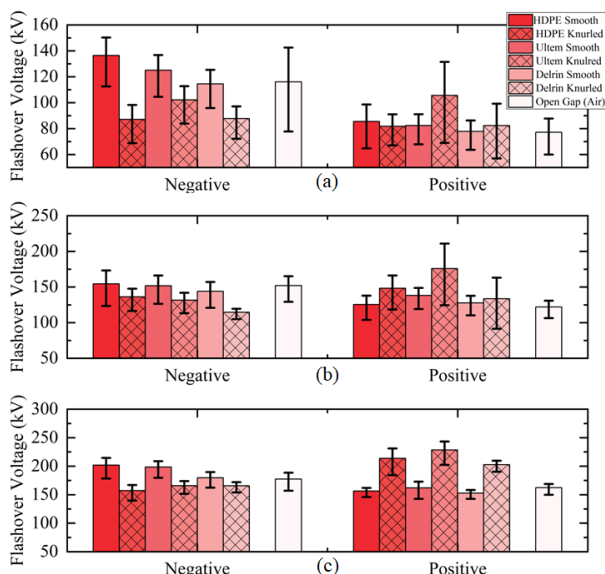


Fig. 6. U_{50} flashover voltages and error bars representing where $\sim 95.4\%$ of data-points reside for each distribution, for Delrin, Ultem and HDPE samples, with both smooth and knurled surface finishes, under negative and positive polarity, at $<10\%$ RH, and at a pressure of a) -0.5 bar gauge, b) 0 bar gauge and c) 0.5 bar gauge.

Fig. 6a shows the results generated at -0.5 bar gauge. Considering the negative-polarity results, there are decreases in the U_{50} values for the knurled samples compared to the smooth samples, for each material. However, although showing the same general trend, the U_{50} voltages for Ultem and Delrin spacers are closer in magnitude. For positive polarity, there is very little difference between the U_{50} breakdown voltages for samples of the same materials with different surface finishes; there is a marginal increase in U_{50} for the Ultem spacer with a knurled finish compared to the smooth Ultem spacer. The open gap results show a higher negative polarity breakdown voltage than positive.

Fig. 6b shows the results at atmospheric pressure (0 bar gauge). For negative polarity, a marginal decrease in the U_{50} breakdown voltage is apparent for the knurled spacers in comparison to the smooth spacers. For positive polarity, similar to the results at -0.5 bar gauge pressure, all materials exhibit similar flashover behaviour, however, differences in the U_{50} flashover voltage values are starting to become apparent, with knurled HDPE and Ultem surfaces reflecting higher U_{50} values than the corresponding smooth surfaces. Similar to the results at -0.5 bar gauge, the negative breakdown voltage is higher than the positive for an open gap. However, the difference between the U_{50} voltages is lower than that at -0.5 bar gauge.

In Fig. 6c, the flashover voltages at 0.5 bar gauge are shown. At this pressure, the widest differences in the U_{50} values for the different insulation systems were observed. For negative polarity, the knurled spacers have lower U_{50} flashover voltages than the corresponding smooth (machined) spacers for HDPE and Ultem, while for Delrin the difference is less pronounced. When the polarity of the impulse is positive, however, there is an opposite effect on the insulation system, where for all materials, knurling the surface is seen to increase the U_{50} flashover voltage, by up to 60 kV, compared to that for a smooth (machined) surface. Again, similar to the results at -0.5 and 0 bar gauge, the negative U_{50} voltage is higher than the positive for an open gap. However, the difference between the negative and positive U_{50} voltages is again reduced compared to the differences seen at lower pressures.

Overall, the similar trends apparent for HDPE, Ultem and Delrin spacers in Figs. 6a, 6b and 6c at the three tested pressures are reflective of the effect the knurling process has on the insulation system. This is hypothesised to be due to competing breakdown mechanisms, resulting in changes to the locations of formation and propagation of the discharge channels at breakdown. The underlying physical mechanisms are discussed in Section IV-B. Additionally, the results in Fig. 6 show that the permittivity of the solid spacers had little effect on the insulation system behaviour under the conditions tested, where comparing flashover voltage distributions of the materials at each test environment exhibited overlapping error bars.

IV. DISCUSSION

The breakdown voltage data, generated in Fig. 6 shows that the spacer surface finish, the air pressure, and the impulse polarity all had an effect on the discharge mechanisms during the flashover process, which could ultimately alter the discharge location. This behaviour is now discussed with reference to the baseline data generated in open air gaps.

A. Open air gap insulation

As shown in Fig. 1b, for the gap spacing and parallel-plane electrodes used here, there is an asymmetrical field distribution within the gap when one electrode is earthed. This phenomenon has been previously discussed in [13], being a result of the ratio of the inter-electrode gap to the radius of the electrode edge. Asymmetric electric field distributions in (geometrically) symmetrical electrode arrangements have also been witnessed by researchers investigating sphere gaps in [15], toroidal electrodes in [16], and for a plane-parallel setup in [17]. In each case, one electrode is earthed, which ultimately leads to a polarity effect when testing with both positive and negative voltages. Referring to the electrostatic simulation in Fig. 1b, it was determined here that for the parallel-plane electrode system used in this paper, where the field at the HV electrode edge is 100% greater than the average field (V/d) in the 40 mm gap, and the electric field at the HV electrode is 87% higher than that at the earthed electrode. This non-uniformity leads to higher negative breakdown voltages, as negative streamers advance due to a rapid outwards acceleration of the electrons constituting the streamer head, creating numerous electron avalanches directed away from the HV electrode [18]. There will be regions of relatively slow-moving positive ions in the tail of the avalanche, in the region near the HV electrode. Also, as electrons are injected, the electronegative nature of the oxygen molecules in air will lead to the attachment of some of these electrons, forming negative ions, reducing the electron population, and meaning that a higher applied field is required to initiate breakdown. Positive streamers, on the other hand, propagate as a result of electron attraction to the positively-charged streamer head, leaving behind regions of positive space charge in the gas, which in this case will increase the local electric field in the gap, increasing the probability of ionisation events occurring in the gap, as the anode has essentially been extended due to the positive ion population, [18]. This increase in local electric field in the gap leads to positive breakdown occurring at lower voltages in bulk air. This explains the lower positive breakdown voltages when discharging across the rounded electrode edges in open air gaps and in air-solid insulation systems with smooth (machined) surfaces, shown in Fig.6.

However, from Fig. 6, it is clear that changing the pressure has an effect on the electrical asymmetry of the system, where the higher the pressure, the more electrically symmetrical the system behaves (the differences between corresponding negative and positive U_{50} values are lower at 0.5 bar gauge than at the lower pressures). This effect is hypothesised as being due to the charge left behind in filaments by incomplete streamers that do not bridge the inter-electrode gap during applied impulses that did not result in breakdown within the step-up testing process. This residual charge may contribute to the polarity effect as the pressure is increased. An example of the visualisation of such streamers in a sphere-sphere topology (lightning impulsive breakdown of air) and the corresponding current waveforms can be found in [19]. The symmetry (or lack thereof) between the positive and negative breakdown voltages, therefore, could be due to the intensity of the pre-breakdown streamers. In [19], streamers were observed to emerge from

both spheres. When the applied voltage was 200 kV, an asymmetry in the positive and negative streamer currents was measured, with the magnitude of the negative current being ~ 5 times less than that of the positive, whereas for 240 kV applied voltage, the currents associated with the negative and positive streamers were equal in magnitude.

The observed reduction in the difference between positive and negative U_{50} values at the higher breakdown voltages measured at 0.5 bar gauge in Fig. 6c, in comparison to the wider differences at -0.5 bar gauge (Fig. 6a) and 0 bar gauge (Fig. 6b), could be a result of (nominally) equally intensive, in terms of streamer current, similar to processes in [19], for positive and negative streamers propagating simultaneously in the inter-electrode gap, with positive and negative charge injected by these streamers. Pressure has been shown to have an effect on breakdown voltage polarity in other research, such as in [17], as the pressure was increased from ~ 0.345 bar to ~ 1 bar (5 to 15 psi in [17]).

B. Air-solid insulation systems

The TJP angle is known to have a large effect on the electric field intensity in a gas-solid insulation system [20]. In the present study, where the contact angle at the TJP was defined by knurling the surfaces of solid samples, the initiation of discharges from two different areas of the electrodes were promoted under different conditions, as shown in Fig. 7.



Fig. 7. Open shutter photographs showing post-breakdown channel location for: a) a smooth (machined) Ultem surface, and b) a knurled Ultem surface.

In the case of a smooth (machined) Ultem surface, breakdown always occurred through the air, initiating and ending at the electrode edges (Fig.7a). However, when a knurled Ultem sample was placed between the electrodes, the dominant breakdown path was across the Ultem/air interface. In this case, as shown in Fig. 2 for contact angles smaller than 56° (for a knurled Ultem) the field at the triple junction exceeds the field at the rounded edge of the upper electrode, promoting a surface flashover across solid/air interface, Fig.7b. The discharge post-breakdown plasma channel closely coupled to the surface of the insulator in this case.

1) Smooth (machined) Surfaces

In terms of the initiation and termination of discharge channels, for a smooth (machined) surface, the plasma channel was located at the outer electrode edge for all breakdowns, irrespective of polarity and material, as shown in Fig. 7a. This is due to the shallow triple junction point angle resulting in the highest electric field residing at the rounded edge of the electrode as shown from Fig. 2. This behaviour manifests in the similar U_{50} voltages for air-solid insulation systems with

smooth (machined) surfaces and the corresponding open-air gap in Fig. 6, with similar processes governing the breakdown event discussed in Section IV A, showing that the relative permittivity of the solid has little effect on U_{50} for these conditions, as the tests exhibit overlapping error bars..

2) Knurled Surfaces

For knurled surfaces, the behaviour of the insulation system is more complex, with the occurrence of discharges closely coupled to the (knurled) sample surface (Fig. 7b) due to the high electric field regions produced as shown from the changing TPJ point angle in Fig. 2., as well as discharges propagating between the electrode edges (Fig 7a). Viewing the experimental results reported here as a whole, encompassing breakdown voltage data and the visual observations, it is clear that the process of knurling the sample surfaces can result in an increased positive U_{50} flashover voltage for certain environmental conditions, linked with a change in the discharge mechanism. This indicates the occurrence of competing breakdown mechanisms, where discharges are initiated at both the high field region associated with the TJP and that associated with the electrode edge. One of these discharges will bridge the gap first leading to breakdown. Researchers in [21] showed that the addition of a screening electrode can increase the breakdown voltage when surface flashover and bulk air breakdown processes are competing. This is particularly relevant in relation to the results generated at 0.5 bar gauge in Fig. 6c here, where the positive U_{50} values for knurled surfaces of all tested materials (with different ϵ_r), are higher than those for smooth (machined) surfaces, as well as those for an open-air gap, despite the increasing field at the TJP with increasing ϵ_r . However, the same performance is not seen using negative polarity. To explain this, the differences between the positive and negative flashover processes have to be discussed, where the mechanisms of positive and negative streamer growth and propagation are different when in the vicinity of a dielectric surface. For this comparison, discharges initiating and propagating in the vicinity of a dielectric surface, as in the case of knurled surfaces in this study, it also has to be considered that the spacer surface itself can be an efficient source of free electrons [22]. Given that positive streamers need free electrons some distance ahead in order to propagate to the point of breakdown [23], and that the efficiency of secondary electron emission (SEE) could be limited, [9], by insulator surface roughness, in this case knurling, if the streamer is following the surface closely, the knurling will affect the length of the streamer, which will be required to propagate a longer distance. The results in an increased voltage drop along the streamer length, reducing the voltage at the streamer front and results in a reduction in the energy available to drive ionisation, [24]. This effect could increase the positive-polarity flashover voltage, which corresponds with empirical data found in this work. Additionally, electrons produced over the surface of the material from SEE processes, and electrons produced through photoionisation at the head of the streamer in the bulk gas which are not adsorbed to the dielectric surface, will expand, and further weaken the electric field at the positive streamer head, [25]. Due to the weakening of the electric field, this will require

a higher applied voltage being required to initiate flashover, than across a non-profiled surface. This effect of positive streamer development has been seen in previous research on profiled dielectric surfaces tested under positive polarity impulse voltages, [26], where discharges were observed by a high-speed camera to propagate only partially across insulator surfaces. For the formation of negative streamers, however, they do not rely as much on adsorbed electrons from the gas-solid interface, where any electrons which are adsorbed by the surface will have little effect of the field at the front of the streamer as the electrons emanate from the streamer head in the gas/solid interface, manifesting in a lower applied voltage to initiate flashover.

To explain the higher positive breakdown voltages in the case of knurled dielectric spacers, as compared with smooth spacers and open-air breakdown voltages, the following hypothesis is proposed. Due to the plasma streamer(s) propagating some distance over the dielectric surface, similar to as shown in [26], the electric field in the whole system can be re-distributed resulting in a decrease in the field on the electrode edge. A 2-dimensional electrostatic model was created using the QuickField finite element solver and the field distribution in the current setup has been obtained in two different cases. The baseline field distribution was obtained for a smooth dielectric, with no streamer(s) in the system. It is shown that the maximum field in this case is achieved at the electrode edge as shown in Fig.1. However, when a streamer starts to propagate across the air/dielectric interface, the field at the electrode edge started to reduce. The streamer initiated at the triple junction was modelled as a 1 mm diameter conducting channel which is attached to the high voltage electrode and this channel (streamer) is at the same potential as the HV electrode. As the streamer increases in length, (l_p), at the dielectric surface, this results in a decrease in the field at the electrode edge by 6% at $l_p = 10$ mm, 18% at $l_p = 20$ mm and 23% at $l_p = 30$ mm in comparison to a 'no streamer' electric field distribution, reducing the probability for the development of a "competitive" streamer(s) which can cross the gap through the air. Thus, in the case of the knurled surface, the streamer is initiated at the triple junction and propagates across the air/dielectric interface, however its development requires an increased applied voltage as the streamer will have a longer length (compared with the case of the smooth spacer) and larger voltage drop across its "body". This increases the breakdown/flashover voltage of the insulation system, leading to either an eventual flashover over the full surface of the knurled insulator, or breakdown in bulk air at the electrode edge (both at a higher applied voltage), giving a potential reason for the higher positive U_{50} for knurled surfaces compared to for smooth surfaces and open-air gaps.

In terms of air pressure, the U_{50} flashover voltages for knurled surfaces are shown to be higher than those for smooth surfaces at 0 bar gauge pressure, as seen in Fig. 6b, and at 0.5 bar gauge pressure, as seen in Fig. 6c. There is clearly less of an effect at -0.5 bar gauge, in Fig 6a. A potential reason for this is that, as the pressure increases, the discharge tends to initiate closer to the TJP, as discussed in [27]. Based upon this, it is hypothesised that the development of positive and negative streamer discharges in the vicinity of dielectric surfaces is affected in different ways. The development of positive

streamers is further impeded by the knurled surface with increasing pressure, due to the aforementioned mechanisms of positive discharges near dielectric surfaces, decreasing the field at the head of the streamer. However, as negative discharges are wider and more diffuse, as discussed in [26], and with electrons emanating from the streamer head, there is minimal effect of the field at the front of the negative streamer, so therefore, the pressure, and the initial location of the discharge at the TJP has little effect on the flashover voltage.

VI. CONCLUSIONS

This paper has reported the impulsive high-voltage testing of electrode-spacer arrangements in dry (<10% RH) air under multiple different conditions, where different materials, surface finishes, and environmental parameters were varied, with a view to providing insights into the flashover processes relevant to the insulation of pulsed power systems operating in environments with fluctuating pressure. It was shown in this work that by modifying (knurling) the spacer surface alone, for all three materials, the flashover voltage increased in comparison to that for the corresponding smooth (machined) spacer, and even an open-air gap, by up to 60 kV at 0.5 bar gauge pressure, under positive polarity energisation.

It was found that at 0.5 bar gauge pressure, under negative polarity, the highest U_{50} values were recorded for spacers with smooth (machined) surfaces, in particular HDPE and Ultem, whereas for positive energisation, the highest breakdown voltages recorded were for knurled spacers, in particular for those made from Ultem.

At 0 bar gauge, for both positive and negative polarity impulses, all materials reflected similar performance in the insulation system, irrespective of surface finish. The results show that, within the conditions tested here, smooth HDPE surfaces are the best choice for negative polarity, while knurled Ultem surfaces offer the highest breakdown voltages for positive polarity.

At -0.5 bar gauge, where the applied impulses were of negative polarity, smooth (machined) spacers were found to have the highest hold-off voltages overall, with HDPE being the best choice of material of those tested. For positive polarity, all materials showed similar flashover voltages irrespective of spacer surface finish, with knurled Ultem surfaces reflecting the highest U_{50} flashover voltage.

The results have demonstrated that modifying physical factors (material, surface finish, and impulse polarity) as well as pressure can have a significant impact on the effectiveness of a composite insulation system, for operation under pulsed power conditions. The results presented herein detail the behaviour of spacers made from three different materials under varied environmental conditions, enabling designers to select the best solution for their application and operational conditions.

ACKNOWLEDGMENT

The authors would like to acknowledge Andy Carlin, Sean Doak, and Louis Cooper from the HVT Mechanical Workshop, Dept of Electronic and Electrical Engineering, University of

Strathclyde, for their assistance with the manufacturing of the solid dielectric samples, electrodes, and test cells.

REFERENCES

- [1] J. D. Smith and L. L. Hatfield, "Measurement of the effects of surface roughness on flashover," 1988. Annual Report., Conference on Electrical Insulation and Dielectric Phenomena, 1988, pp. 47-52, doi: 10.1109/CEIDP.1988.26307.
- [2] J. O. Rossi, M. Ueda, A. R. Silva and L. P. S. Neto, "Improvement on UHMWPE and PMMA Surface Flashover Under Atmospheric Pressure Using PIII Processing," in IEEE Transactions on Plasma Science, vol. 48, no. 10, pp. 3386-3391, Oct. 2020, doi: 10.1109/TPS.2020.3007735.
- [3] M. Dhofir, R. N. Hasanah and H. Suyono, "The Leakage Current and Flashover Voltage of Polyethylene Insulator with Different Contour Surfaces," 2020 12th International Conference on Electrical Engineering (ICEENG), 2020, pp. 17-22, doi: 10.1109/ICEENG45378.2020.9171763.
- [4] L. LIU et al., "The Influence of Electric Field Distribution on Insulator Surface Flashover," 2018 IEEE Conference on Electrical Insulation and Dielectric Phenomena (CEIDP), 2018, pp. 255-258, doi: 10.1109/CEIDP.2018.8544732.
- [5] H. - Lee, T. Egashira and M. Hara, "Improvement of particle-initiated DC flashover characteristics by using electrode and surface shapes in SF6 gas," [1991] Proceedings of the 3rd International Conference on Properties and Applications of Dielectric Materials, 1991, pp. 529-532 vol.1, doi: 10.1109/ICPADM.1991.172114
- [6] C. Sun et al., "Characteristics of nanosecond pulse dielectric surface flashover in high pressure SF6," in IEEE Transactions on Dielectrics and Electrical Insulation, vol. 25, no. 4, pp. 1387-1392, August 2018, doi: 10.1109/TDEL.2018.006759
- [7] X. Yang et al., "Research on forming mechanism of surface discharge paths for solid dielectric with different shapes under micro-second impulse in liquid nitrogen," in IEEE Transactions on Dielectrics and Electrical Insulation, vol. 24, no. 6, pp. 3452-3459, Dec. 2017, doi: 10.1109/TDEL.2017.006769.
- [8] J. Xue, H. Wang, J. Chen, K. Li, Y. Liu, B. Song, J. Deng, and G. Zhang, "Effects of surface roughness on surface charge accumulation characteristics and surface flashover performance of alumina-filled epoxy resin spacers", Journal of Applied Physics 124, 083302 2018 <https://doi.org/10.1063/1.5043239>
- [9] P. Xue, S. Zhao, D. Xiao, L. Zhu and Y. Wu, "Experimental Research on Flashover Characteristics of Insulator with N2," in IEEE Electrical Insulation Conference (EIC), San Antonio, TX, 2018, pp. 60-63. doi: 10.1109/EIC.2018.8480897.
- [10] Y. Qin et al., "A Study on Flashover Characteristics of Supporting Insulators in SF6 under Lightning Impulse," in IEEE 11th International Conference on the Properties and Applications of Dielectric Materials (ICPADM). Page 604 – 607, 2015 doi: 10.1109/ICPADM.2015.7295344.
- [11] Z. Jia, B. Zhang, X. Tan and Q. Zhang, "Flashover Characteristics along the Insulator in SF6 Gas under DC Voltage," 2009 Asia-Pacific Power and Energy Engineering Conference, Wuhan, China, 2009, pp. 1-4, doi: 10.1109/APPEEC.2009.4918383.
- [12] ASTM D3426-97 Standard Test Method for Dielectric Breakdown Voltage and Dielectric Strength of Solid Electrical Insulating Materials Using Impulse Waves
- [13] R. W. Macpherson, M. P. Wilson, I. V. Timoshkin, S. J. Macgregor and M. J. Given, "Impulsive Flashover Characteristics and Weibull Statistical Analysis of Gas-Solid Interfaces with Varying Relative Humidity," in IEEE Access, vol. 8, pp. 228454-228465, 2020, doi: 10.1109/ACCESS.2020.3046088
- [14] N. Enkhmunkh, G. Won Kim, K. Hwang and S. Hyun, "A parameter estimation of Weibull distribution for reliability assessment with limited failure data," 2007 International Forum on Strategic Technology, 2007, pp. 39-42, doi: 10.1109/IFOST.2007.4798514.
- [15] R. Arora and W. Mosch, "The Effects of Grounding on Field Configuration", in *High Voltage and Electrical Insulation Engineering*, Wiley IEEE Press Series on Power Engineering, Piscataway NJ, 2011
- [16] A. Pokryvailo, "Calculation of breakdown voltage of gas gaps with arbitrary geometry on examples of spheres and toroids," 2017 IEEE 21st International Conference on Pulsed Power (PPC), Brighton, UK, 2017, pp. 1-4, doi: 10.1109/PPC.2017.8291190.
- [17] V. K. Gandhi, R. Verma, M. Warriar, and A. Sharma, "Effect of Electrode Profile and Polarity on Performance of Pressurized Sparkgap Switch"

Plasma 5, no. 1, 2020, pp. 130-145.
<https://doi.org/10.3390/plasma5010010>.

- [18] J. M. Meek and J. D. Craggs, "Electrical Breakdown of Gases". London: Clarendon Press, 1953.
- [19] V. A. Chirkov, A. V. Samusenko, and Y. K. Stishkov, "Current pulses caused by streamers in sphere-sphere electrode system", in *Journal of Physics Conference Series*, 2015, vol. 646, no. 1. doi:10.1088/1742-6596/646/1/012042.
- [20] H. C. Miller, "Surface flashover of insulators," in *IEEE Transactions on Electrical Insulation*, vol. 24, no. 5, pp. 765-786, Oct. 1989, doi: 10.1109/14.42158.
- [21] A. Xu, Y. Shi, Y. Cheng and L. Chen, "Influence of Screening Electrode on Surface Flashover in Atmospheric Environment," in *IEEE Transactions on Dielectrics and Electrical Insulation*, vol. 30, no. 2, pp. 580-584, April 2023, doi: 10.1109/TDEI.2023.3235309.
- [22] M. Akyuz, L. Gao, V. Cooray, T. G. Gustavsson, S. M. Gubanski, and A. Larsson, "Positive streamer discharges along insulating surfaces," *IEEE Transactions on Dielectrics and Electrical Insulation*, vol. 8, no. 6, pp. 902-910, 2001.. doi: 10.1109/94.971444.
- [23] A. A. Dubinova, "Modeling of streamer discharges near dielectrics", Doctor of Philosophy, Applied Physics and Science Education, University of Eindhoven 2016.
- [24] H. K. H. Meyer, R. Marskar, H. Gjerdal and, F. Mauseth "Streamer propagation Along a Profiled Dielectric Surface" in *Plasma Sources Sciences and Technology*, vol 29, no 11 pp. 115015, 2020, doi: 10.1088/1361-6595/abbac2
- [25] F. Wang, L. Wang, S. Chen, Q. Sun and L. Zhong, "Effect of Profiled Surface on Streamer Propagation and the Corner Effect," in *IEEE Transactions on Dielectrics and Electrical Insulation*, vol. 28, no. 6, pp. 2186-2194, December 2021, doi: 10.1109/TDEI.2021.009866.
- [26] H. K. Meyer, R. Marskar, H. Osberg and F. Mauseth, "Surface Flashover over a Micro-Profiled Cylinder in Air," in *IEEE Transactions on Dielectrics and Electrical Insulation*, doi: 10.1109/TDEI.2023.3277413
- [27] C. Tran Duy, N. Bonifaci, A. Denat, O. Lesaint, L. Caliap, A. Girodet, B. Gelloz, P. Ponchon, "Partial discharges at a triple junction metal/solid insulator/gas and simulation of inception voltage", *Journal of Electrostatics*, VI 66, Is. 5-6, 2008, pp. 319-327, <https://doi.org/10.1016/j.elstat.2008.01.011>



Ruairidh W. Macpherson (M'23) was born in Inverness, Scotland, in 1990. He received his B.Eng. (Hons.), and MPhil degrees from the University of Strathclyde in 2016 and 2019, respectively. Where he is currently working as an RA and pursuing his Ph.D. degree with the High Voltage Technologies Group, Department of Electronic and Electrical Engineering. His research interests include work in pulsed power, corona-stabilized switches, environmentally friendly gas dielectrics, surface flashover of gas-solid interfaces within sub-optimal environmental conditions and HVAC, HVDC and impulsive plasma characterisation.



Mark P. Wilson (M'10) was born in Stranraer, Scotland, in 1982. He received the B.Eng. (with honours), M.Phil., and Ph.D. degrees in electronic and electrical engineering from the University of Strathclyde, Glasgow, U.K., in 2004, 2007, and 2011, respectively. He is presently based in the High Voltage Technologies research group at the University of Strathclyde, where his research interests include interfacial surface flashover, nanodielectrics, and the practical applications of high power ultrasound, corona discharges, and pulsed electric fields. Mark is a member of the IEEE Nuclear and Plasma Sciences Society, from whom he received a Graduate Scholarship Award in 2011, the IEEE Dielectrics and Electrical Insulation Society, and the IET.



Igor V. Timoshkin (M'07-SM'14) received the degree in physics from Moscow State University, Moscow, Russia, in 1992, and the Ph.D. degree from the Imperial College of Science, Technology, and Medicine (ICSTM), London, U.K., in 2001. He was a Researcher with Moscow State Agro-Engineering University, Moscow, and the Institute for High Temperatures of the Russian Academy of Sciences, Moscow. In 1997, he joined ICSTM. He joined the Department of Electronic and Electrical Engineering, University of Strathclyde, Glasgow, U.K., in 2001, where he became a Reader in 2016. His research interests include dielectric materials, pulsed power, transient spark discharges, and environmental applications of non-thermal plasma discharges. Dr. Timoshkin was a Voting Member of the Pulsed Power Science and Technology Committee in the IEEE Nuclear and Plasma Science Society (2017-2021); currently he is a member of the International Advisory Committee of the IEEE Conference on Dielectric Liquids and the International Scientific Committee of the Gas Discharges and their Applications Conference; a Subject Editor of IET Nanodielectrics and a member of the Editorial Board of MDPI Energies.



Martin J. Given (M'99-SM'11) is currently a Senior Lecturer in the Department of Electronic and Electrical Engineering at the University of Strathclyde. He received a degree in physics from the University of Sussex in 1981 and a PhD in electronic and electrical engineering from the University of Strathclyde in 1996. His research interests include, ageing processes and condition monitoring in solid and liquid insulation systems, high speed switching and pulse power applications. fundamental study of plasma sources, and fabrication of micro- or nanostructured surfaces.



Scott J. MacGregor (M'95-SM'14) received the B.Sc. and Ph.D. degrees from the University of Strathclyde, Glasgow, U.K., in 1982 and 1986, respectively. He became a Pulsed Power Research Fellow in 1986 and a Lecturer in pulsed-power technology in 1989. In 1994, he became a Senior Lecturer, with a promotion to Reader and Professor of High Voltage Engineering, in 1999 and 2001, respectively. In 2006 and 2010 he became Head of the Department of Electronic and Electrical Engineering and Executive Dean of the Faculty of Engineering and has been the Vice-Principal of the University of Strathclyde since 2014. Professor MacGregor was the recipient of the 2013 IEEE Peter Haas Award, and he was appointed as an Associate Editor of the *IEEE Transactions on Dielectrics and Electrical Insulation* in 2015. His research interests include high-voltage pulse generation, high-frequency diagnostics, high-power repetitive switching, high-speed switching, electronic methods for food pasteurisation and sterilisation, generation of high-power ultrasound (HPU), plasma channel drilling, pulsed-plasma cleaning of pipes, and stimulation of oil wells with HPU.